Check for updates

Dendrimersome Synthetic Cells Harbor Cell Division Machinery of Bacteria

Anna M. Wagner, Hiromune Eto, Anton Joseph, Shunshi Kohyama, Tamás Haraszti, Ricardo A. Zamora, Mariia Vorobii, Marina I. Giannotti, Petra Schwille,* and Cesar Rodriguez-Emmenegger*

The integration of active cell machinery with synthetic building blocks is the bridge toward developing synthetic cells with biological functions and beyond. Self-replication is one of the most important tasks of living systems, and various complex machineries exist to execute it. In *Escherichia coli*, a contractile division ring is positioned to mid-cell by concentration oscillations of self-organizing proteins (MinCDE), where it severs membrane and cell wall. So far, the reconstitution of any cell division machinery has exclusively been tied to liposomes. Here, the reconstitution of a rudimentary bacterial divisome in fully synthetic bicomponent dendrimersomes is shown. By tuning the membrane composition, the interaction of biological machinery with synthetic membranes can be tailored to reproduce its dynamic behavior. This constitutes an important breakthrough in the assembly of synthetic cells with biological elements, as tuning of membrane–divisome interactions is the key to engineering emergent biological behavior from the bottom-up.

1. Introduction

One of the ultimate goals of bottom-up synthetic biology has been to design and create a fully synthetic protocell. Such artificial cells should contain key aspects of biological behavior, such as compartmentalization, transport of molecules, metabolism, growth, and ideally, replication through cell division. The latter is one of the hallmarks of life and one of the most intriguing phenomena exhibited by living organisms.[1] Beyond that, synthetic cells could comprise features that biological ones lack, such as an increased stability against environmental conditions, or much simplified programmability for desired new functions to be utilized in (bio)technological applications.[2]

One obvious strategy for designing such hybrid protocells includes encapsulating components of the active cell machinery into artificial cell-like compartments. The most prominent methods involve the use of liposomes, which are lipid bilayer compartments that mimic cells with respect to their size and provide basic biochemical functionalities.[3] In these systems, reconstitution of minimal components of cell division has been demonstrated.[3b] A notable example is the MinCDE protein system, which is the spatial regulator of cell division for many

A. M. Wagner, A. Joseph, T. Haraszti, M. Vorobii,
C. Rodriguez-Emmenegger
DWI–Leibniz Institute for Interactive Materials
Forckenbeckstraße 50, 52074 Aachen, Germany
E-mail: rodriguez@dwi.rwth-aachen.de

A. M. Wagner, A. Joseph
Institute of Technical and Macromolecular Chemistry
RWTH Aachen University
Worringerweg 2, 52074 Aachen, Germany

H. Eto, S. Kohyama, P. Schwille
Max Planck Institute of Biochemistry
Department of Cellular and Molecular Biophysics
Am Klopferspitz 18, 82152 Martinsried, Germany
E-mail: schwille@biochem.mpg.de

R. A. Zamora, M. I. Giannotti, C. Rodriguez-Emmenegger
Institute for Bioengineering of Catalonia (IBEC)
The Barcelona Institute of Science and Technology (BIST)
Carrer de Baldiri Reixac 10-12, Barcelona 08028, Spain
E-mail: crodriguez@ibecbarcelona.eu

R. A. Zamora, M. I. Giannotti
Network Biomedical Research Center on Bioengineering
Biomaterials and Nanomedicine (CIBER-BBN)
Madrid 28029, Spain

M. I. Giannotti
University of Barcelona
Department of Materials Science and Physical Chemistry
Martí i Franquès 10, Barcelona 08028, Spain

C. Rodriguez-Emmenegger
Institució Catalana de Recerca i Estudis Avançats (ICREA)
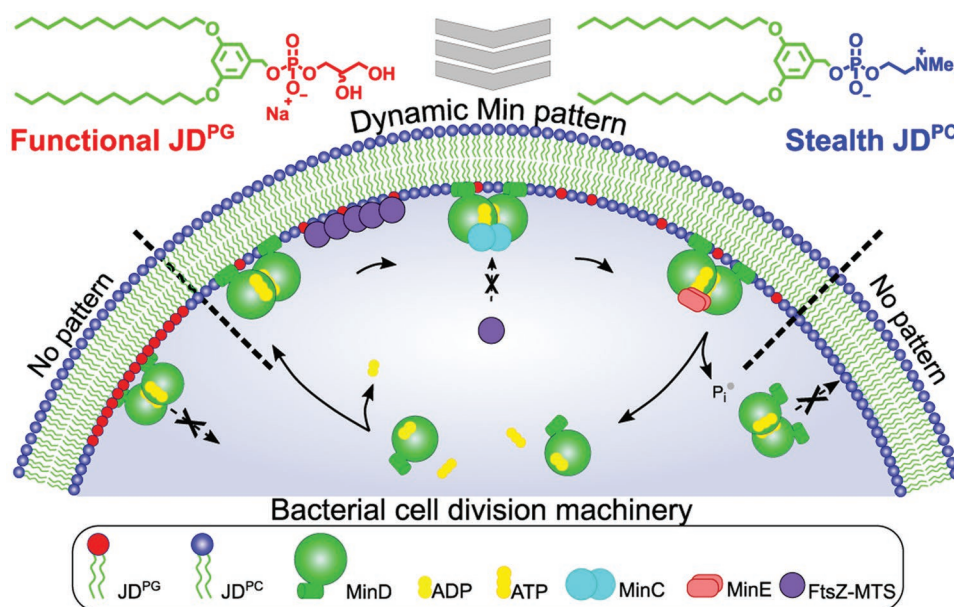Passeig Lluís Companys 23, Barcelona 08010, Spain

Figure 1. Schematic representation of the synchronization of interactions between a fully synthetic DS membrane and active cell division machinery. By varying the JD^{PG}:JD^{PC} ratio (decreasing clockwise) the Min protein pattern can be programmed from irreversible binding (left) or no attraction (right) to a dynamic pattern formation (center) to recapitulate the behavior in living systems.

bacterial species, establishing symmetrical cell division.[4] In *Escherichia coli*, these proteins direct the assembly of FtsZ protein filaments at mid-cell through periodic pole-to-pole oscillations, where they form a proto-ring that subsequently recruits further proteins of the divisome.[5] A key feature of Min proteins is that they self-organize into dynamic patterns, whose behavior is delicately governed by the interplay between the diffusion and kinetic rates of the molecules between the intracellular spaces and the membrane.[6] In this regard, liposomes are suitable model membrane systems to recapitulate such protein behaviors in vitro. However, the self-organization into protein patterns is not necessarily restricted to liposomes. Using only natural components precludes our ability to evolve synthetic cells artificially for non-natural functions. It is the integration of active cell machinery, perfected by evolution over millennia, with synthetic macromolecular and supramolecular building blocks that put these extremely complex tasks within reach. Rationally designed and well-defined functional building blocks can be synthesized with a tailored interactivity holding the key to a higher level of biomimicry. But can we reconstitute the active cell division machinery in biomembranes assembled from synthetic molecules that do not exist in nature? This will demand a precise balance of strength and dynamics of interactions between the synthetic membrane and the components of the bacterial cell division machinery.

One state-of-the-art synthetic membrane system are polymersomes assembled from amphiphilic block copolymers.[7] The vast choice of monomers and synthetic routes enable designing and controlling the surface topology of the vesicle and the generation of reactive nano- and microdomains.[8] The enhanced stability is a consequence of the molecular organization, which comes at the cost of a greater thickness that negatively affects the insertion of the positioning system of the divisome.[7e,9] Concurrently, the entanglement of the hydrophobic chains results in slower dynamics (viscosity, diffusion, flip-flop)[10] that severely hamper their ability to be synchronized with a dynamic reaction–diffusion system as the MinCDE positioning system. This significantly hinders the insertion of membrane proteins and the mimicry of functions that demand remodeling of the membrane, such as division.[7a,c,e,9b,11] We therefore developed a vesicle system to reconstitute the cell division machinery and to probe how the strength of interaction between the membrane and the Min positioning system controls the dynamic behavior. Our fully xenobiotic system is based on dendrimersomes (DSs) assembled from amphiphilic Janus dendrimers (JDs).[12] Such membranes have superior mechanical and chemical stability compared to liposomes,[12,13] and they are particularly attractive because of their facile, modular synthesis, which enables us to introduce structural and functional variability[9a,14] to precisely program tailored multivalent interactions with proteins and cells.[15] Indeed, the fine tuning of biophysical parameters, such as membrane thickness, flexibility, lateral mobility, and permeability, as well as the biochemical functionalities, is crucial for recreating an artificial membrane suitable for the integration of protein systems.[16] This is one of the main reasons why the in vitro reconstitution of many protein systems has only been successfully performed on lipid membranes and has been a prominent limitation for other synthetic membrane systems such as polymersomes.[7e,9]

In this work, we synthesized JDs designed to mimic fundamental properties and functions of natural cell membranes. One molecule (JD^{PC}) contains a zwitterionic phosphocholine headgroup that renders the membrane stealth to proteins,[17] while the other has a phosphoglycerol headgroup (JD^{PG}) for the tuning of attractive interactions that is crucial for many bacterial proteins to function, including the Min and FtsZ proteins (**Figure 1**).[6a] The strength of interactions could be tuned by the ratio of the JDs and the emergence of dynamic protein patterns could be programmed within an optimized range of ratios. We
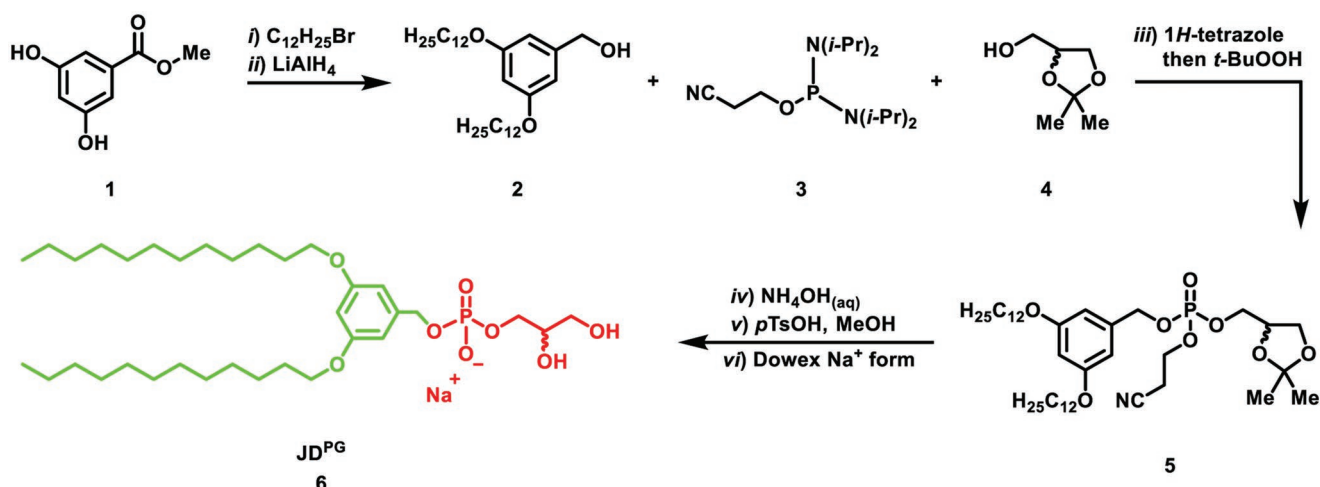
Figure 2. Synthesis of JD^PG: i) 1, $C_{12}H_{25}Br$, K_2CO_3, DMF, 80 °C, 24 h; ii), $LiAlH_4$, THF, 0 °C to room temperature (r.t.), 24 h; iii) 2, 3, 4, ^1H-tetrazole, MeCN, CH_2Cl_2, r.t., 17 h then t-BuOOH$_{(aq)}$, r.t., 1 h; iv) 5, $NH_4OH_{(aq)}$, MeOH, r.t., 2 h, v) pTsOH, MeOH, 40 °C, 4 h; vi) Dowex Na^+ form, MeOH, r.t., 4 h.

rigorously tested the evolution of dynamic behavior by forming a variety of model membrane systems: supported membranes, water-in-oil droplets, and vesicles,[3b] and studied their interaction with the *E. coli* MinDE system. Not only did the proteins form dynamic patterns, but they also showed remarkably similar behavior as observed on lipid membranes. We also co-encapsulated Min and FtsZ proteins in DSs, where formation and location of FtsZ filaments were spatially regulated by Min proteins. Thus, it was possible to synchronize the interactions of a natural system with a fully synthetic one and reproduce the emergent behavior, representing the first example of active cell division machinery successfully incorporated into a fully synthetic vesicle. The modularity of our synthetic system is the key to introduce further active cell machineries to develop synthetic cells that are coming closer and closer to living ones.

2. Results and Discussion

2.1. Design and Synthesis of Janus Dendrimers

JD^PC was selected as a structural component due to its ability to form biomimetic membranes. JD^PG was synthesized (**Figure 2**; Synthesis, Figures S1–S3, Supporting Information) to introduce attraction to the membrane targeting domains of the divisome components and therefore must homogeneously mix with JD^PC to form membranes where we can continuously tune the attraction. This was programmed by choosing the same hydrophobic 3,5-didodecyloxylbenzylic dendron for both JDs. The hydrophobic part is designed to yield an increased stability in the resulting DSs, as compared to liposomes, while maintaining the thickness of natural membranes. The hydrophobic dendron was synthesized by an etherification of 3,5-dihydroxybenzoate (**1**) with 1-bromodecane and subsequent reduction to (3,5-didodecoxyphenyl)methanol (**2**). For the synthesis of JD^PG (**6**), phosphordiamidite chemistry was employed to couple the hydrophobic dendron **2** and solketal **4** to bis(diisopropylamino)(2-cyanoethoxy)phosphine (**3**). Subsequent oxidation with t-BuOOH yielded the desired phosphate **5**. After alkaline

removal of the 2-cyanoethyl protecting group and subsequent acid-catalyzed deprotection of the acetonide group, the resulting product was treated with Na^+ ion exchange resin to obtain the desired JD^PG in 22% yield with regard to the hydrophobic dendron **2**.

2.2. Self-Assembly of Janus Dendrimers into Biomimetic Dendrimersomes

JDs were self-assembled into DS vesicles by the thin-film-rehydration method. This method yields giant unilamellar vesicles (2–50 μm in diameter) as observed by confocal laser scanning microscopy (CLSM). The membrane thickness (3.7 ± 0.4 nm) was determined by analysis of deposited vesicles in atomic force microscopy (AFM) (Figure S4, Supporting Information). The height and phase images by AFM revealed completely homogeneous membranes for all studied ratios of JD^PG: JD^PC, demonstrating that both JDs homogeneously mix in any ratio of concentrations (**Figure 3**a). Such mixing is a sine qua non condition for the continuous tuning of interactions. We determined the diffusion coefficients and mobile fractions (Figure S5, Supporting Information) for JD and lipid membranes by fluorescence recovery after photobleaching (FRAP) (Figure 3b). The latter membranes consist of DOPC/DOPG, which are a model of *E. coli* membranes. Fast dynamics were observed for both systems in agreement with being above their melting temperature (–14 and –17 °C for JD^PC and JD^PG, respectively). The diffusion coefficients (D) were maximal for supported bilayers of the pure JD^PC or DOPC (2.7 ± 0.8 μm² s⁻¹ and 2.5 ± 1.8 μm² s⁻¹, respectively) and decreased monotonically with increasing ratio (10–40 mol%) of the negatively charged functional components. This trend may be associated with a stronger association of the negatively charged amphiphiles with the underlying substrate and a concomitant reduction of their mobility. However, even the lowest diffusion coefficients are ≈10–1000 times higher than for polymersomes.[10a,11b,18] The drastic difference between the D of polymersomes and the ones liposomes and dendrimersomes stems from their completely different molecular arrangement.
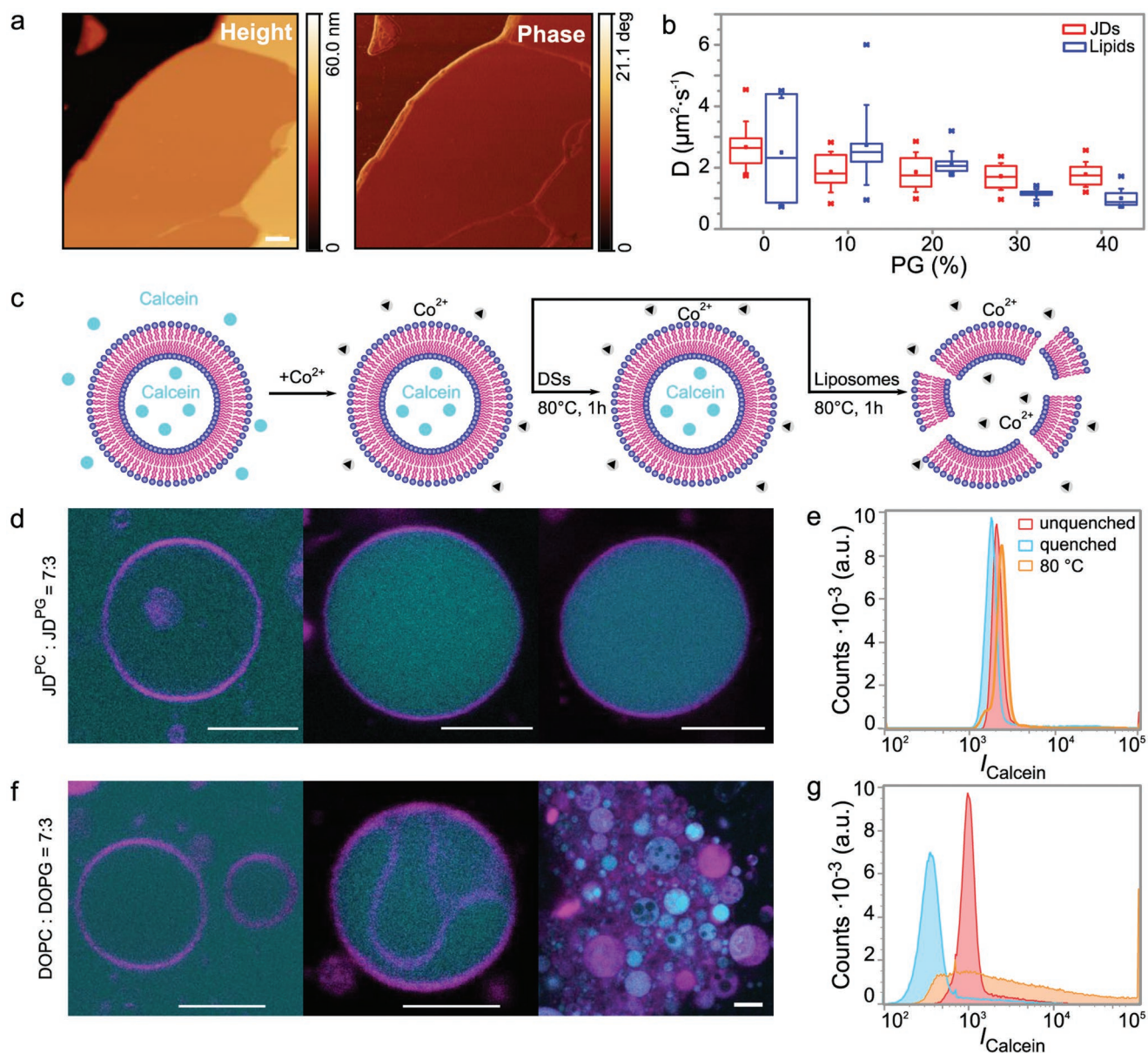
ADVANCED
SCIENCE NEWS
www.advancedsciencenews.com

ADVANCED
MATERIALS
www.advmat.de

Figure 3. Characterization of dendrimersomes compared to liposomes. a) Surface topography from AFM analysis of DS vesicles (JD^PC: JD^PG 7:3) in height (left) and phase (right) revealed homogeneous mixing. Scale bar: 200 nm. b) Determination of diffusion coefficients for supported bilayers formed from JDs and lipids with varying composition measured by FRAP. The boxes range from the 25th to the 75th percentile of each data set where the median is depicted by a line and the average value by an open rectangle. Each box was obtained from ten data points. The whiskers show the standard deviation with outliers outside of the whiskers. c) Scheme of the qualitative assessment of stability and permeability. Vesicles were formed in a calcein solution. In a second step Co^{2+} was added to the outside solution to quench calcein fluorescence. Then the vesicles were heated to a temperature of 80 °C for 1 h and cooled down before measurement. DS vesicles remain intact while liposomes undergo breakage and aggregation upon heating. d,f) Each step is depicted in CLSM snapshots for dendrimersomes (d) and liposomes (f) with e,g) the respective quantitative assessment of membrane stability by FACS after the same steps for dendrimersomes (e) and for liposomes (g). The membranes were labeled with 0.1 mol% Nile red (magenta) and filled with calcein (cyan). Scale bars: 10 μm.

In polymersomes, D is controlled by the motion of the entangled hydrophobic blocks that follow either the Rouse or reptation models.[10a] Such motion is much slower and rapidly decreases with molecular weight. On the other hand, the hydrophobic tails in lipids or dendrimersomes are not entangled, thus the motion only requires to exchange positions and is therefore much faster. The temperature stability of DSs and liposomes

was assessed by CLSM and fluorescence activated cell sorting (FACS) (Figure 3c). Addition of Co^{2+} to calcein-filled DSs did not change the fluorescence intensity in the vesicle lumen demonstrating impermeability of the membrane to ions. Contrarily, a decrease in fluorescence was observed for liposomes indicating a permeable membrane. When DSs were heated to 80 °C they remained stable (Figure 3d,e) while liposomes

**ADVANCED
SCIENCE NEWS**
www.advancedsciencenews.com

**ADVANCED
MATERIALS**
www.advmat.de

underwent membrane breakage and aggregation (Figure 3f,g). Moreover, addition of α-hemolysin to DSs resulted in rapid quenching (Figure S6, Supporting Information) meaning that the pore forming peptide could insert into the membrane, diffuse within the membrane, and assemble into a pore highlighting the biomimicry of our synthetic system. Furthermore, the DS membranes could withstand indentation forces almost twice as large as DOPC/DOPG membranes when indented by the AFM probe[19] (Figure S7, Supporting Information) demonstrating a superior mechanical stability.

Although the chemical structure of the JDs significantly differs from their natural counterparts, synthetic DSs display a high level of biomimicry with a biomimetic thickness, a high lateral mobility while having a more stable membrane. As a result, these vesicles can unite the most important physical properties of liposomes such as thickness, flexibility, lateral mobility, and permeability with the superior mechanical and chemical stability of polymersomes.

2.3. Dynamic Self-Organization Patterns of MinDE Proteins on Supported Janus Dendrimer Membranes

We assessed the generation of self-organized dynamic patterns of membrane-associating MinD and MinE proteins on supported dendrimer bilayers (SDBs). The formation of protein patterns is a consequence of the reaction–diffusion mechanism of both proteins that associate with the membrane (**Figure 4**a).[6a] MinD has an amphipathic and positively charged helix (membrane targeting sequence, MTS) with low affinity toward the membrane.[20] However, upon binding of ATP, MinD dimerizes enabling the binding to the membrane. The strength of binding increases with the coulombic attraction to the negatively charged membrane lipids and by higher order lateral interactions with other MinD dimers.[21] Stable pattern formation relies on these higher order interactions, which require membranes with high lateral mobility to enable the lateral associations within MinD dimers.[21a] Membrane-bound MinD recruits MinE to the surface, which concomitantly activates MinD ATPase activity. Hydrolysis of the bound ATP switches MinD to its monomeric state, which is followed by its detachment from the membrane.[22] After detachment, MinE lingers on the membrane that prevents rapid MinD reattachment.[21b] Thus, the formation of dynamic Min patterns requires a precise tuning of the interactions between proteins and membrane (Figure 1).

MinD formed a homogeneous protein coat when added together with ATP to JD^{PC}: JD^{PG} 7:3 SDBs (Figure S8, Supporting Information). Further addition of MinE turned the coat into dynamic traveling waves that emerged in a wide range of conditions with varying protein concentration and
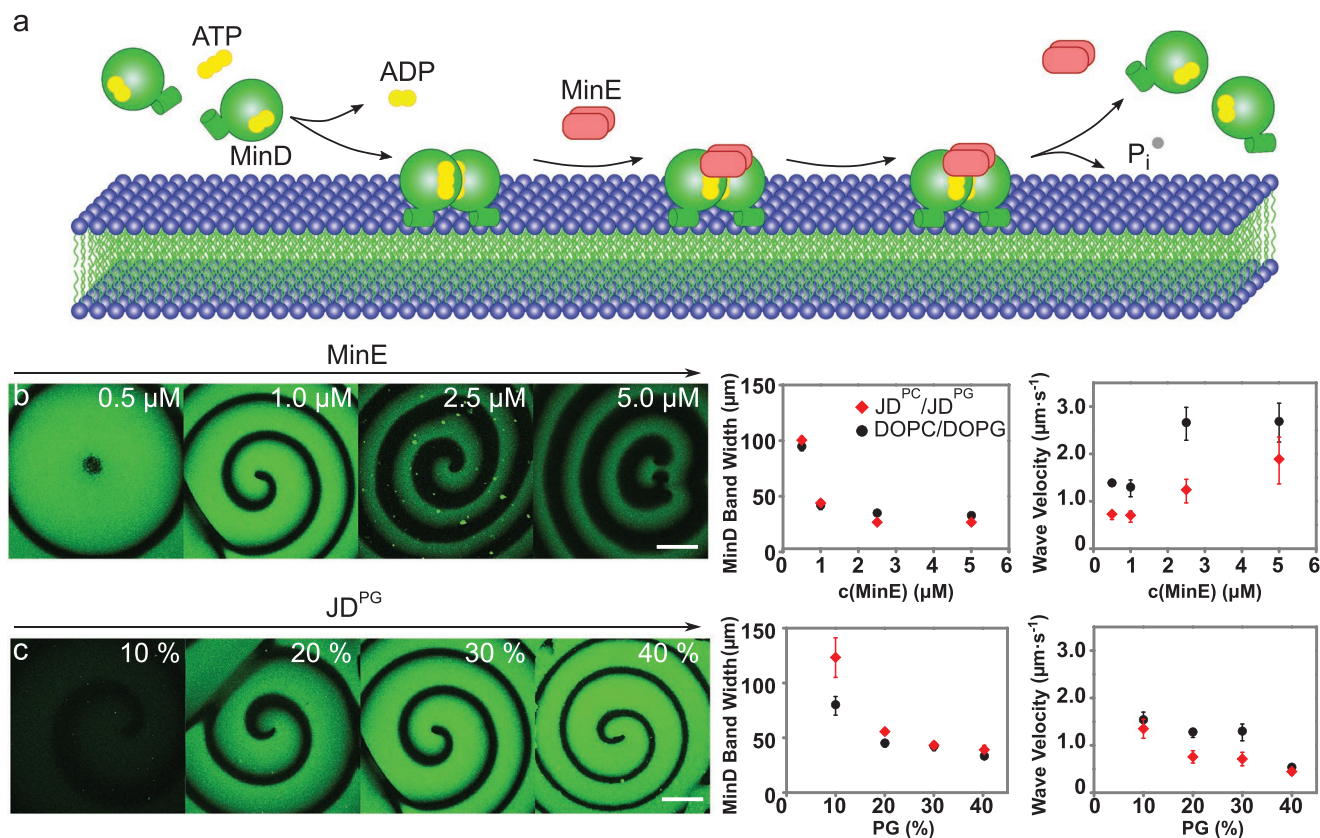

Figure 4. MinDE self-organization patterns on supported dendrimer membranes. a) Scheme of MinDE reaction–diffusion mechanism. b) Dynamic traveling waves with increasing MinE concentration (0.5–5 × 10⁻⁶ M MinE, 1 × 10⁻⁶ M MinD, JD^{PC}: JD^{PG} 7:3). Plots of bandwidth (left) and wave velocity (right) against MinE concentration of JD and lipid membranes. c) Dynamic traveling waves with increasing PG content (10–40% PG, 1 × 10⁻⁶ M MinD and MinE). Plots of wave bandwidth (left) and wave velocity (right) against PG content in JD and lipid membranes. Each data point has been obtained from n = 3 independent measurements. The error bars indicate the standard deviation. Scale bar: 50 μm.

membrane composition. First, we varied the MinE concentration (0.5–5 × 10⁻⁶ ᴍ MinE) at a constant MinD concentration resulting in traveling waves spanning over several millimeters (Figure 4b; Videos S1 and S9–S11, Supporting Information). For SDBs, the MinD bandwidth closely resembled the ones obtained for lipids decreasing from 99 µm (94 µm in SLBs) for the lowest MinE concentration to 27 µm (32 µm in SLBs) for the highest MinE concentration. Wave velocity in SDB, on the other hand, increased with increasing concentration of MinE following a similar trend as SLBs. It increased from 0.7 µm s⁻¹ (1.4 µm s⁻¹ in SLBs) for the lowest MinE concentration to 1.9 µm s⁻¹ (2.7 µm s⁻¹ in SLBs) for the highest MinE concentration. Increasing the concentration of MinE leads to a higher rate of MinD detachment and prevents the rapid reattachment of MinD, concomitantly resulting in narrower bands. On the other hand, this faster exchange of proteins led to a more rapid increase in frequency and thereby an increase in the wave velocity.

Furthermore, we varied the membrane content of JD^PG (0–40%) to tune the density of negative charge on the SDBs (Figure 4c; Video S2, Supporting Information). No pattern formation was observed when the bilayers were formed only from the electroneutral JD^PC. Increasing the ratio of JD^PG and the negative charge, the fluorescence intensity increased since more MinD binds to the membrane. The MinD bandwidth decreased from 123 µm (79 µm in SLBs) for 10 mol% PG to 39 µm (32 µm in SLBs) for 40 mol% PG. Simultaneously, the wave velocity follows the same trend decreasing from 1.3 µm s⁻¹ (1.5 µm s⁻¹ in SLBs) for the lowest PG concentration to 0.4 µm s⁻¹ (0.5 µm s⁻¹ in SLBs) for the highest PG concentration. A higher density of negative charge promotes more binding of MinD, which recruits a higher concentration of MinE to the membrane. After MinD detachment, MinE lingers on the membrane consistent with a decreasing MinD bandwidth. Concurrently, the dynamics of the waves become slower due to a locally higher density of MinD bound to the substrate.

Remarkably, the SDBs faithfully recapitulated the trends of the dynamic properties observed for SLBs of related chemical structures (Figure S11, Supporting Information) demonstrating that JD^PC: JD^PG are synthetic surrogates of lipids.

2.4. Compartmentalization of MinDE in Synthetic Janus Dendrimer Droplets and Dendrimersomes

We studied the emergence of dynamic behavior of the MinDE system inside droplets and vesicles assembled from synthetic JDs. Since the lipid composition DOPC: DOPG 7:3 mimics *E. coli* membranes,[21b] we chose JD^PC: JD^PG 7:3 as the optimum composition. The simplest 3D spherical compartment that allows to study the spatiotemporal MinDE dynamics are water-in-oil emulsion microdroplets with their characteristic monolayer interface oriented between an inner water and outer oil phase (**Figure 5**a).[23] The encapsulation of MinDE proteins into JD droplets successfully demonstrated the formation of waves (Figure S12, Supporting Information) supporting the hypothesis that a JD monolayer is sufficient for the peripheral insertion of the amphipathic helix (MTS) of MinD[23a] and the preservation of Min oscillations under 3D confinement.

However, toward the development of synthetic cells, the encapsulation of functional biomolecules into vesicles is a more
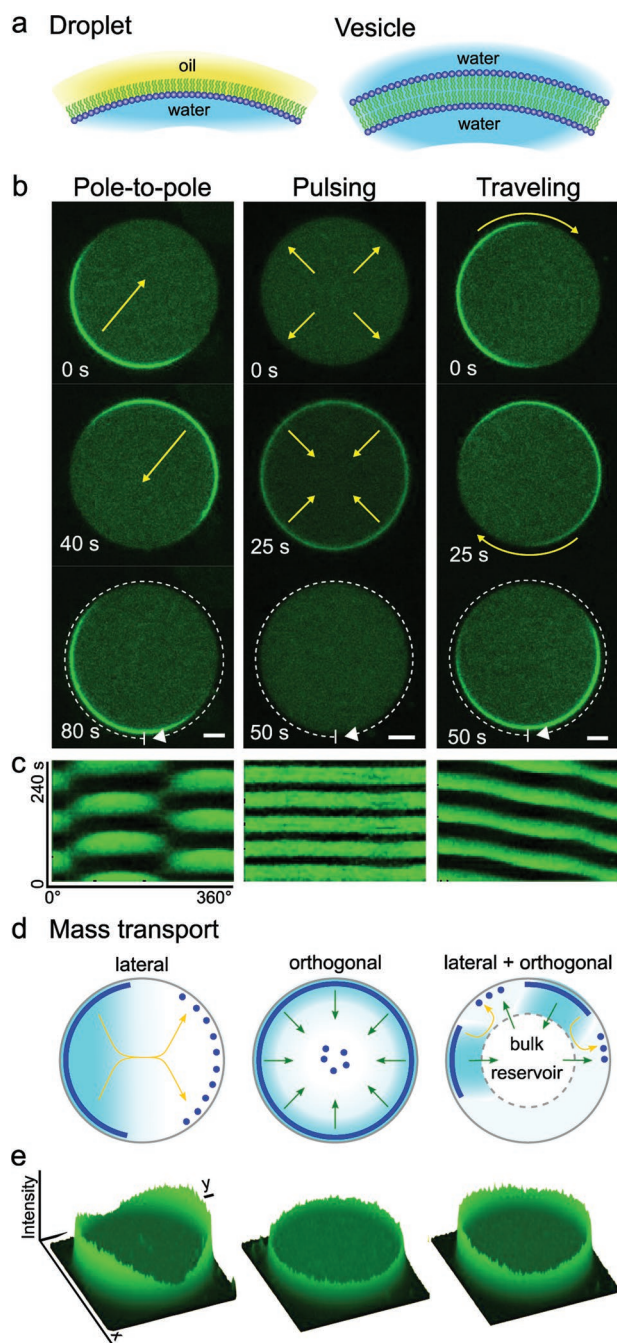

Figure 5. Encapsulation of MinDE into compartments assembled from JDs. a) Scheme of the interface of droplets and vesicles depicting molecular organization. b) CLSM snapshots of pole-to-pole, pulsing and traveling oscillations in dendrimersomes with c) Kymographs taken along the indicated white dotted line. d) Scheme of the mechanism of mass transport for the three modes of oscillation. e) 2D time-averaged fluorescence intensity of MinD-eGFP in dendrimersomes. MinD 1 × 10⁻⁶ ᴍ (30% of MinD was fused to eGFP), MinE 0.5 × 10⁻⁶ ᴍ. Scale bar: 5 µm.

general model system wherein the membrane not only functions as a compartment but actively transforms in response to reactions from within.[24] Therefore, we prepared vesicles with encapsulated MinDE proteins by the water-in-oil emulsion-transfer method.[23a,25] Remarkably, compartmentalization of the Min proteins in microdroplets and vesicles gave rise to

spatiotemporal patterns described by three separate modes: i) pole-to-pole, ii) pulsing, and iii) traveling waves with their respective characteristic kymographs (Figure 5b,c; Videos S3–S5, Supporting Information).

In pole-to-pole oscillations, Min proteins are cyclically oscillating from one pole of the compartment to the other, generating the highest temporal-average protein density at both poles. These oscillations are dominated by a lateral mass transport along the membrane, which requires a sufficiently small volume to generate a membrane-bulk gradient that drives the alternating binding (Figure 5d,e).[26] The pole-to-pole oscillation naturally occurs in *E. coli*.[27] However, in this experimental model the volume-to-area is larger than in the bacterium, which allows additional modes of dynamic oscillation such as pulsing and traveling waves. These modes have been previously reported inside lipid compartments.[23,26,28] In large vesicles, the mass transport orthogonal to the membrane may become dominant over the lateral one. This gives rise to the pulsing mode, where Min proteins oscillate between the bulk and the membrane.[23,26,28] Due to the antiphase coupling of attachment and detachment oscillation, the time-averaged protein density at the whole membrane remains constant with a higher intensity compared to the more diluted protein concentration in the lumen (Figure 5e). The third mode consists of a circular wave propagating with a constant time-averaged protein density at the membrane. The mechanism involves the superposition of both lateral and orthogonal mass transport leading to the decoupling of membrane and bulk and the formation of a bulk reservoir.[26] Such a superposition results in traveling waves, analogous to the protein patterns, and kymographs previously observed on SDBs and SLBs with an infinite bulk reservoir (Figure 4; Figure S10, Supporting Information). The surface plots confirm a higher density of proteins at the membrane and an overall lower concentration of proteins in the lumen compared to the pulsing mode.

The simultaneous existence of the three different modes of oscillation has been firstly reported for liposomes and is a manifestation of the multistability of the system.[26,28] It was shown that the patterns largely depend inter alia on protein concentrations, cell geometry, and bulk volume, where smaller bulk volumes tend to favor the characteristic in vivo pole-to-pole oscillations by suppressing orthogonal mass transport modes.[23b,26] In liposomes, the oscillations have characteristic periods between 40 and 120 s.[6b] Similarly, the oscillation period in dendrimersome vesicles varied from 80 s (50 s in droplets) for pole-to-pole, 50 s (30 s in droplets) for pulsing to 60 s (60 s in droplets) for traveling modes. The presence of the modes and similarity in their dynamic behavior evidences that the interfaces formed by JDs represent functional analogous models to lipid compartments.

2.5. Assembly and Regulation of a Division Ring in Synthetic Dendrimersomes

To probe the faithful biomimicry of our membranes, we reconstituted a minimal divisome based on FtsZ, and its regulation system based on Min proteins within DS vesicles. Bacterial cell division is initiated by the assembly of FtsZ proteins into ring-shaped filaments at mid-cell.[5b] Structured FtsZ filaments

are precursors of the Z-ring, followed by the assembly of other division-related proteins into a cell division complex, a so-called divisome.[29] Highly controlled spatial positioning of the FtsZ proteins is regulated by MinC proteins that colocalize with MinD oscillation and act as the negative regulator of FtsZ assembly, i.e., prevent their binding to the membrane.[27,30] Therefore, the simultaneous reconstitution of FtsZ and MinCDE within vesicles is a key step toward the construction of a divisome in synthetic and hybrid cells.

To minimize the complexity of the system, we employed four proteins, MinCDE and FtsZ-MTS. The latter is a chimeric FtsZ fused to MinD's C-terminus MTS region that is capable of binding FtsZ to the membrane without the need of additional adaptor proteins.[5b] Confocal microscopy images (**Figure 6**b) and Z-scans (Figure S13, Supporting Information) showed that FtsZ-MTS assembled into filaments nucleated at the DSs membrane. These filaments formed a network that counter-oscillates with MinC as observed in kymographs and the time-evolution of the protein density (Figure 6c; Video S6, Supporting Information). This antagonistic behavior of MinC and the branched network of FtsZ filaments demonstrate that the positioning and regulatory functions of the MinCDE system could indeed be recapitulated in our xenobiotic DSs. This level of biomimicry has, to our knowledge, not been accomplished by other families of synthetic vesicles, such as polymersomes. This demonstrates that the combination of cells parts and machinery with DSs is a promising new strategy toward creating synthetic cells in vitro, by not only mimicking the cellular membrane functions, but also beyond them.

3. Conclusions

This work demonstrates the successful reconstitution of an active bacterial divisome in fully synthetic vesicles by programming the strength and dynamics of membrane–divisome interactions. We designed new types of Janus dendrimers (JD^{PC}, JD^{PG}) that assembled into dendrimersomes with a high level of biomimicry. The tuning of the JD^{PC}: JD^{PG} ratio allowed the emergence of dynamic Min patterns on SDBs. Remarkably, the dynamic patterns closely resembled those observed for analogous lipid compositions. When compartmentalized into DSs, three modes of Min oscillations were obtained: i) pole-to-pole, ii) pulsing and (iii) traveling waves, with the first one being characteristic for living cells. The Min system could direct the dynamic assembly and positioning of FtsZ filaments at the membrane. Thus, this demonstrates that the synchronization of the interactions between synthetic and natural systems is the key to replicate the emergent behavior pervasive in life.

4. Experimental Section

Statistical Analysis: All of the reported experiments were performed at least twice to confirm the reproducibility of the results. All directly measured data were presented without preprocessing unless stated otherwise. All boxplots were generated from 10 data points containing 25–75% of the data set. In Figure 3d–f and Figure S6b,c (Supporting Information) single representative vesicles are shown in CLSM while in Figure 3e–g and Figure S6d (Supporting Information) quantitative characterization was done in FACS with 15 000 events per sample. Each
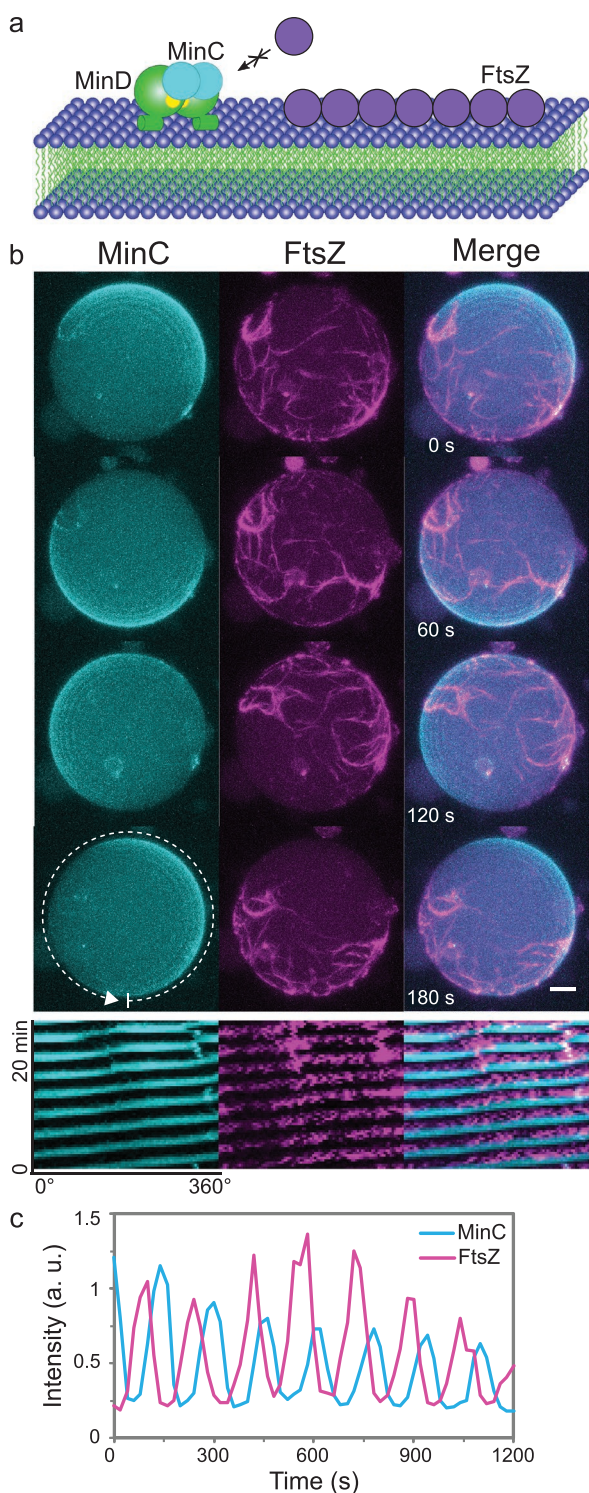
Figure 6. Dynamic assembly of FtsZ filaments by the encapsulation of MinCDE and FtsZ-MTS proteins into DSs. a) Mechanism of MinC-FtsZ interactions. b) Maximum intensity projection of DSs with labeled MinC (cyan) and FtsZ (magenta). Time-lapse images and kymographs taken from the indicated white dotted line shows that FtsZ counter-oscillates with MinC. c) Time evolution of protein density. 0.5×10^{-6} M mCherry-MinC, 2×10^{-6} M FtsZ-YFP-MTS, MinD 1×10^{-6} M, MinE 0.5×10^{-6} M. Scale bar: 5 μm.

data point from the statistical data shown in Figure 4b,c was obtained from $n = 3$ independent measurements. Data were expressed as mean ± standard deviation. All data were processed according to the description in the respective Supporting Information Section. Statistical analysis and data fitting were performed in OriginPro2018, Python, and R.

Supporting Information

Supporting Information is available from the Wiley Online Library or from the author.

Conflict of Interest

The authors declare no conflict of interest.

Author Contributions

A.M.W. and H.E. contributed equally to this work. C.R.E. and P.S. jointly supervised the project. A.M.W., H.E., A.J., M.V., C.R.E., and P.S. designed the experiments. A.J. synthesized the Janus dendrimers. A.M.W. and T.H. carried out the self-assembly studies and the membrane characterization. H.E. analyzed the FRAP data and R.A.Z. and M.I.G. performed and analyzed the AFM force spectroscopy experiments. A.M.W. and H.E. performed the Min protein in vitro reconstitution experiments. A.M.W., H.E., and S.K. performed encapsulation experiments in droplets and vesicles and analyzed the data. A.M.W. and S.K. designed the figures. A.M.W. and C.R.E. wrote the paper with contributions from all authors.

Data Availability Statement

The data that support the findings of this study are available from the corresponding author upon reasonable request.